# STUDIES OF THE EARTH'S OUTER RADIATION ZONE

D. J. Williams

On Sept. 28, 1963, this Laboratory launched into a nearly circular polar orbit a research satellite containing charged-particle detectors designed to measure the spatial and temporal properties of the earth's radiation zones.

Several APL studies concerning trapped electrons have now been completed, using the data from this satellite. Included in these studies is an investigation of the characteristics and decay of the artificial radiation belt that had been created by the high-altitude nuclear detonation of July 9, 1962.[1] In addition to providing valuable information concerning loss mechanisms (the source function is essentially zero) these results are valuable to the payload engineer so that he may more accurately estimate satellite dose rates caused by the trapped radiation. Both the observed decay of the artificial radiation zone and its dependence on geomagnetic position and particle energy have been incorporated into a computer program that yields for the design engineer estimates of the expected dose rate in any desired orbit.

Another investigation concerns the observation of trapped electrons being lost in the atmosphere as they drift into the South Atlantic Anomaly (a region of very low magnetic field strength in the South Atlantic). Of further interest in this study

[1] C. O. Bostrom and D. J. Williams, "Time Decay of the Artificial Radiation Belt," *J. Geophys. Res.*, **70**, 1965, 240–242.

*Data from the APL satellite* 1963 38C *have provided much useful information concerning the earth's radiation belts. In particular, studies relating to the outer radiation zone indicate that the behavior of high-energy electrons in this region in magnetically quiet periods is consistent with their movement in a distorted magnetic field under the conservation of adiabatic invariants. Furthermore, it has been possible to obtain a magnetic field configuration that can explain the observed electron movements. These investigations are described in this article.*

is the observed replenishment of electrons to these trapping regions at longitudes well removed from the Anomaly. These results are particularly interesting as they represent a slow but steady leak for the entire geomagnetically trapped particle population.[2]

Further studies indicative of the intimate connection, through the solar wind-magnetospheric interaction, between geomagnetically trapped particles and interplanetary conditions, include observation of a direct correlation between trapped electron intensities in the outer zone and magnetic activity.[3] This study has also yielded trapping lifetime and response times to magnetic disturbances as a function of both electron energy and position within the magnetosphere.

Further evidence of the above solar-terrestrial relationship is the discovery of a striking correlation of the trapped electron intensities throughout the outer zone with the solar rotation period of $\approx 27$ days.[4] These intensity variations appear to be closely related to certain recently reported struc-

[2] D. J. Williams and J. W. Kohl, "Loss and Replenishment of Electrons at Middle Latitudes and High B Values," to be published Sept. 1, 1965, *J. Geophys. Res.*

[3] D. J. Williams and A. M. Smith, "Daytime Trapped Electron Intensities at High Latitudes at 1100 Kilometers," *J. Geophys. Res.*, **70**, 1965, 541–556.

[4] D. J. Williams, "Outer Zone Electrons," Paper presented at the Advanced Study Institute, "Radiation Trapped in the Earth's Magnetic Field," Bergen, Norway, Aug. 16 – Sept. 3, 1965.

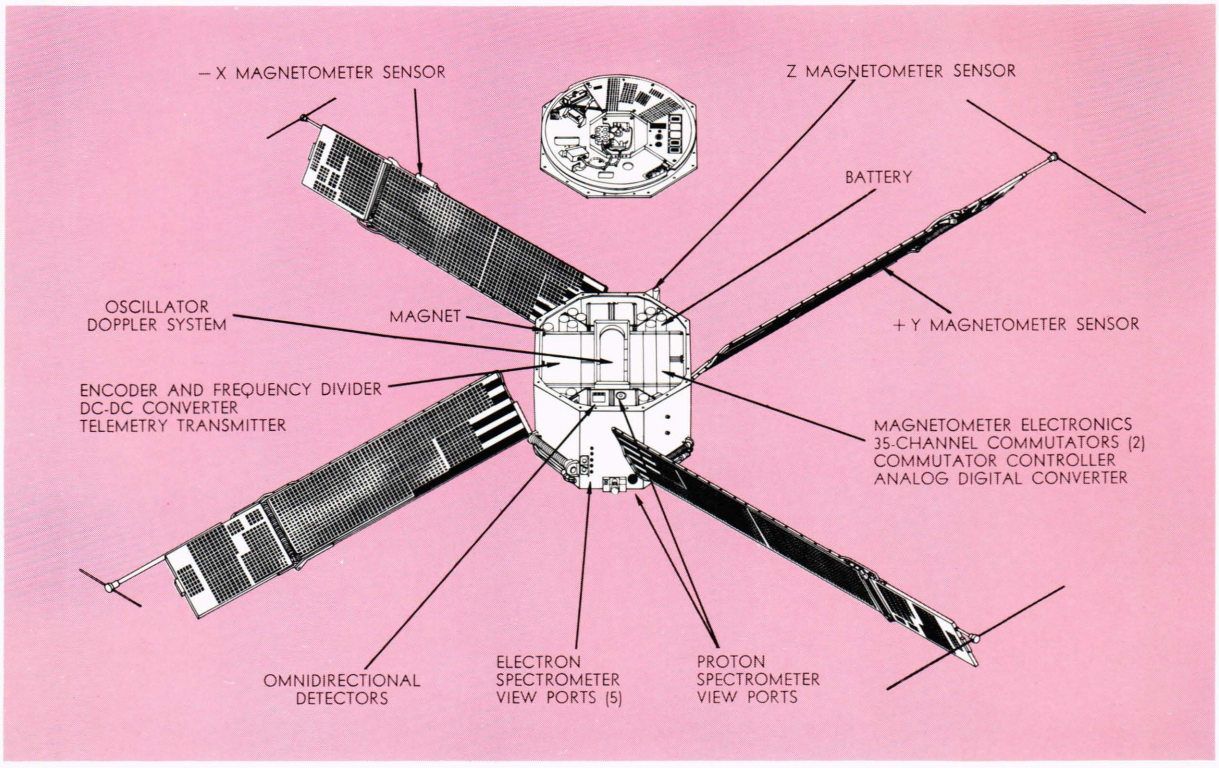


**Fig. 1—A diagrammatic view of APL Satellite *1963 38C*.**

tural components of the interplanetary magnetic field.[5]

An early study pertaining to the solar wind-magnetospheric interaction was the measurement of a significant diurnal variation of trapped electrons in the outer radiation zone and their temporal behavior. The early analysis of this effect suggested that it might be explained by magnetospheric distortions caused by the incident solar wind.[6]

Of concern in this paper are the results of a more recent study in which we have investigated in detail the observed diurnal variations mentioned above. We have found that high-energy electrons behave in a manner consistent with their movement in a distorted magnetosphere under the conservation of energy and certain invariants of the motion. Obtaining constant value contours of these invariants allows us to predict the observed asymmetries in the trapped particle spatial distribution. The invariants of interest are the first and second adiabatic invariants of trapped particle motion. The first or magnetic moment invariant is given by

$$\mu = \frac{p_\perp^2}{2mB} = \frac{p^2}{2mB_m}$$

in its relativistic form. Here $\mu$ = magnetic moment, $p$ = momentum, $p_\perp$ = component of momentum normal to line of force, $m$ = particle mass, $B$ = field strength, and $B_m$ = mirror point field strength. The magnetic moment invariant is associated with a characteristic time equal to the particle gyroperiod about the line of force ($\approx 10^{-5}$ sec for a 100-kev electron near the equator at $L = 2$).

The second or longitudinal invariant is given by

$$J = \int_M^{M^*} p_{||}\, ds,$$

where the line integral is taken along the magnetic line of force between the mirror point $M$ and its conjugate $M^*$. $J$ is associated with a characteristic time equal to the bounce period between conjugate points ($\approx 0.2$ sec for a 100-kev electron near the equator at $L = 2$).

Furthermore, in this study it has been possible to obtain a nightside configuration for the earth's

[5] N. F. Ness and J. M. Wilcox, Goddard Space Flight Center Report No. X-612-65-157, Apr. 1965.

[6] D. J. Williams and W. F. Palmer, "Distortions in the Radiation Cavity as Measured by an 1100 Kilometer Polar Orbiting Satellite," *J. Geophys. Res.*, **70**, 1965, 557-567.

TABLE I
CHARACTERISTICS OF ELECTRON SPECTROMETER, ORIENTED 90° TO SATELLITE ALIGNMENT AXIS

| *Detector* | *Half Angle (degrees)* | *Geometric Factor ($cm^2$ ster)* | *Foil Thickness ($mg/cm^2$)* | *Particle Energies Yielding Pulses Between 250-kev and 1-Mev Discriminator Levels* | |
|---|---|---|---|---|---|
| | | | | *Electrons (Mev)* | *Protons (energies in Mev)* |
| 1 | 6.4 | $2.8(10)^{-3}$ | 10.3 Al | $\geq 0.28$ | $2.0 \leq E_p \leq 2.3$ $\quad E_p \geq 178$ |
| 2 | 6.4 | $2.8(10)^{-3}$ | 412 Cu | $\geq 1.2$ | $14.4 \leq E_p \leq 14.5$ $\quad E_p \geq 179$ |
| 3 | 6.4 | $2.8(10)^{-3}$ | 946 Cu | $\geq 2.4$ | $23.27 \leq E_p \leq 23.34$ $\quad E_p \geq 181$ |
| 4 | 6.4 | $2.8(10)^{-3}$ | 1470 Cu | $\geq 3.6$ | $30.01 \leq E_p \leq 30.07$ $\quad E_p \geq 183$ |
| 5 | 3.2 | $4.9(10)^{-4}$ | 10.3 Al | $\geq 0.28$ | $2.0 \leq E_p \leq 2.3$ $\quad E_p \geq 178$ |

magnetic field by requiring that such a field fit the observed asymmetries in the radiation cavity.[7] These efforts were carried out in conjunction with Dr. G. D. Mead of the Goddard Space Flight Center (NASA), Greenbelt, Maryland.

The APL satellite of interest here bears the international designation *1963 38C*. It achieved a nearly circular polar orbit, with a perigee of 1067 km, an 1140-km apogee, an 89.9° inclination, and a 107.5-min. period. Because of its high inclination the orbital plane is essentially fixed in inertial space and precesses at the approximate rate of 1° per day in an easterly direction with respect to the earth-sun line. Shortly after launch, the satellite orbital plane was at an angle of $\approx 6°$W of the noon-midnight meridian.

Figure 1 is a diagrammatic view of the satellite. Magnetic alignment to a 6° oscillation about the local line of force was achieved about three days after launch. When aligned, the satellite Z-axis points downward over the North Pole.

There are three charged-particle experiments aboard satellite *1963 38C;* a triad of omnidirectional units, sensitive to both electrons and protons, consisting of three 1.5-mm cubic Li-drifted solid-state detectors; a proton spectrometer consisting of two 500-$\mu$ surface-barrier solid-state detectors; and an electron spectrometer consisting of five 1000-$\mu$ surface-barrier solid-state detectors. The satellite and all charged-particle experiments are still operating satisfactorily after 22 months of continuous operation.

## The Experiment

The electron spectrometer was oriented to "look" out normal to the satellite alignment axis; thus, after alignment was achieved, it monitored the intensity of trapped electrons mirroring at the point of observation.

Two discriminator levels, at 250 kev and 1.0 Mev, plus various absorbing foils, yield the characteristics shown in Table I. In the outer radiation zone, proton contamination in the response of the electron spectrometer, as indicated in Table I, is expected to be negligible. Monitoring the proton spectrometer has shown this to be the case.

## Data

In seeking an ambient configuration for the magnetospheric cavity that is consistent with experimental observations, we have used data only from magnetically quiet periods. We have not considered any details of the observed correlation of increases in radiation cavity distortions with increases in magnetospheric distortions, as reported in Ref. 6 for magnetically active periods.

The data are for the relatively quiet period of Oct. 2 through 12, 1963, when the satellite orbital plane was within 8° of the noon-midnight meridian. Some 47 dayside passes and 28 nightside passes, obtained from the NASA receiving stations at College, Alaska, and Winkfield, England, have been analyzed. Little, if any, nightside data are available from the remaining stations in our network.

In Fig. 2 we show composite curves representative of the average trapped electron intensity (count rate) for this time period plotted against invariant magnetic latitude $\Lambda$, where $\cos\Lambda = 1/\sqrt{L}$, and $L$ represents the equatorial crossing distance (in earth radii) of a line of force in a dipole field. Thus $\Lambda$ represents the latitude at which a given line of force intersects the earth's surface. Profiles for both the noon and midnight

[7] D. J. Williams and G. D. Mead, "A Nightside Magnetospheric Configuration as Obtained from Trapped Electrons at 1100 km," *J. Geophys. Res.*, **70**, 3017–3029, 1965.

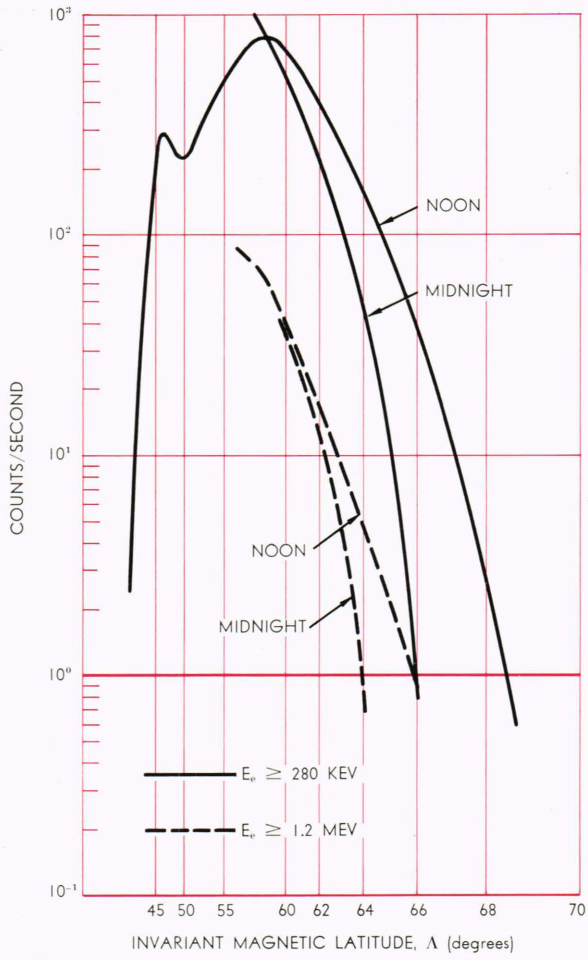


**Fig. 2—Day and night count rate versus Λ curves for the magnetically quiet period Oct. 2-12, 1963. The observed count rate is a measurement of trapped electron intensity and Λ is an invariant magnetic latitude.**

latitudes, $\Lambda_D$ and $\Lambda_N$ respectively, are shown for the electron energies $E_e \geq 280$ kev and $E_e \geq 1.2$ Mev. Flux values (electrons/cm$^2$ sec ster) may be obtained by multiplying the observed count rates by 500 for the $E_e \geq$280-kev channel, and 1000 for the $E_e \geq 1.2$-Mev channel.

It is seen that for both energies the noon and midnight latitude profiles display a clear separation. (In a pure dipole field the latitude profiles at all local times would be expected to be identical.) This separation can have two causes: permanent injection and/or acceleration mechanisms operating on the particles as they drift in the magnetosphere; or a latitude shift of the trapped-electron population caused by the azimuthal drift of these electrons in a distorted magnetosphere under the conservation of the adiabatic invariants.

The first of these mechanisms seems unlikely because of the high electron energies involved and also because no energy dependence in the observed shift has been recorded at these energies. Furthermore, acceleration effects resulting from electric fields associated with daily geomagnetic variations are in the wrong direction and are much too small to cause the effects observed here.

Consequently, we have investigated the possibility of explaining these shifts by particle drift in a distorted magnetosphere under the conservation of the adiabatic invariants (the second mechanism above). To do this we assume that the noon-midnight differences seen in Fig. 2 are caused by a latitude shift of the trapped-electron population as these electrons drift from the noon to the midnight meridian. We then can obtain the dayside and nightside latitudes, $\Lambda_D$ and $\Lambda_N$ respectively, corresponding to a constant trapped-electron intensity. From these values we now plot in Fig. 3 the amount of latitude shift, $\Delta\Lambda = \Lambda_D - \Lambda_N$ observed for these electrons as a function of noon-meridian (dayside) latitude. The data points of Fig. 3 are mean values of all the data obtained, and the bars show the entire spread of values observed during the period under study.

Intermixing of the two energies in Fig. 3 indicates that high-energy electrons in general exhibit a rather well defined behavior in the outer radiation zone during periods of magnetic quiet.

The most accurate data available are those shown in Fig. 3 as matched-pass data. They stem from pairs of passes received at College, Alaska, and Winkfield, England, in which the satellite is continuously observed as it travels from the dayside hemisphere over the North Pole and down the nightside portion of its orbit, or vice versa. Such pairs of passes, being but minutes apart, eliminate a great amount of the scatter caused by magnetic activity. These matched passes are as close as we are able to come to the ideal case of simultaneous observation of the day and nightside latitude profiles.

To use the remaining data and to provide a check on the accuracy of the matched-pass data, daily averaged noon and midnight latitude profiles were obtained for each day of this study period. From these curves the nightside and dayside latitudes corresponding to constant electron intensity were again obtained. In Fig. 3 we also show the mean values of all the daily average data, which, we note, show a bit more scatter than the matched-pass data. This might be expected since the daily average data will be affected by magnetic variations taking place within a 24-hr period, whereas the matched-pass data are affected only

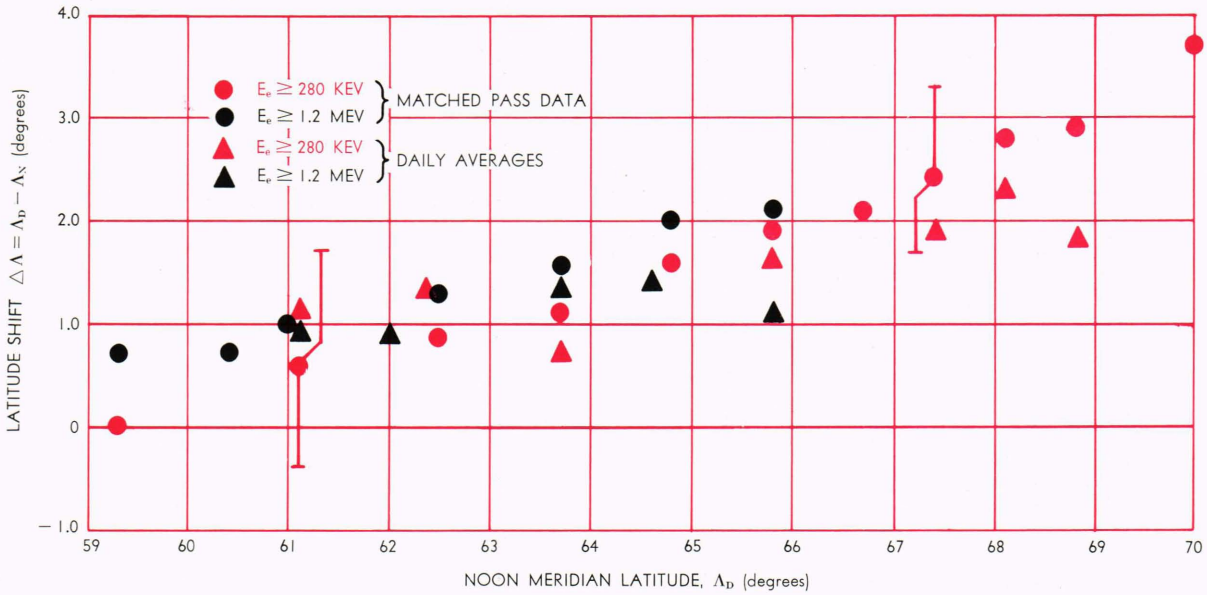


**Fig. 3—Plot showing the amount of latitude shift, $\Delta\Lambda = \Lambda_D - \Lambda_N$, of the trapped electron population as a function of the noon meridian latitude, $\Lambda_D$. Data are mean values and are discussed in the text. The bars show the entire spread of values observed during the period under study.**

by magnetic variations taking place within ≈ 30 min.

## Results

We can now attempt to fit the observed latitude shifts shown in Fig. 3 by using various magnetospheric models and obtaining the particle drift under conservation of the adiabatic invariants.

The magnetospheric model with which we have started is that described by Mead[8] and is shown in Fig. 4. This model is an especially convenient starting point as it presents the magnetic field configuration obtained from the earth's dipole field in the presence of the solar wind (a continuous flow of plasma from the sun). A surface is formed from the solar wind-magnetosphere interaction which, in the absence of other perturbing effects, confines the earth's magnetic field to a finite volume, the magnetospheric cavity. The currents on this surface generally compress the earth's field lines, the compression being much more pronounced on the dayside than on the nightside. Taking into account the flow of plasma around the earth leads to the fact that high-latitude field lines emanating from the sunward hemisphere are actually bent back over the poles and are carried on into the nightside portion of the magnetosphere.

A further convenience of Mead's field is that with a dayside boundary of 10 earth radii, good agreement is obtained with experimental measurements of the field and boundary position on the dayside hemisphere.[9] Therefore, we need only adjust the nightside portion of Fig. 4 to fit the data of Fig. 3.

The indication of plasma currents in the magnetospheric tail (as implied from magnetic-field observations[10]) has led us to consider the follow-

[8] G. D. Mead, "Deformation of the Geomagnetic Field by the Solar Wind," *J. Geophys. Res.*, **69**, 1964, 1181–1195.

[9] N. F. Ness, C. S. Scearce and J. B. Seek, "Initial Results of the IMP 1 Magnetic Field Experiment," *J. Geophys. Res.*, **69**, 1964, 3531–3569.

[10] N. F. Ness, "The Earth's Magnetic Tail," *J. Geophys. Res.*, **70**, 1965, 2989–3005.

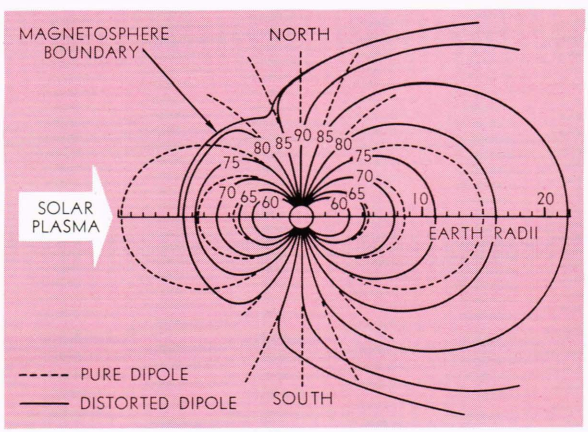


**Fig. 4—Magnetic field configuration in the noon-midnight meridian resulting from the interaction of the earth's dipole field with plasma flowing from the sun. Higher order terms in the earth's field expansion do not materially change the overall configuration shown here. (From Ref. 8, courtesy, *Journal of Geophysical Research.*)**

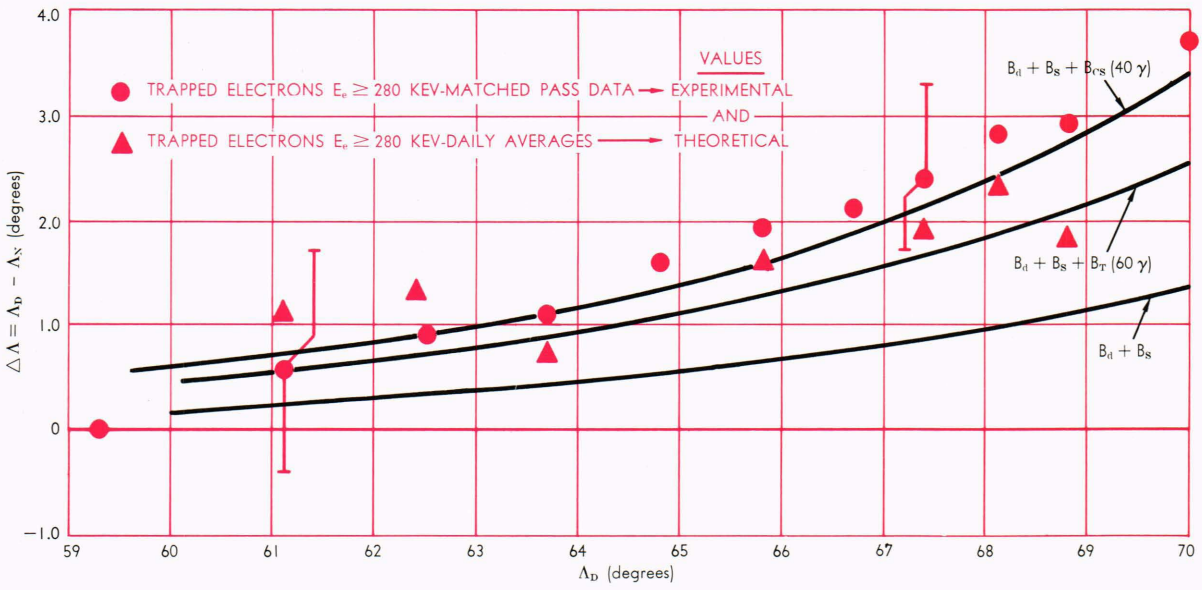


**Fig. 5—Comparison of experimental observations of the latitude shift with expectations of various field models assuming particle drift under conservation of the adiabatic invariants. Solid lines are the result of computations.**

ing two adjustments to the nightside configuration: the addition of a constant-tail field, $B_T$, which is directed away from the sun in the southern hemisphere and toward the sun in the northern hemisphere (this addition corresponds to observed field directions well out in the magnetospheric tail);[10] and the addition of a current sheet lying in the nightside magnetic equatorial plane and extending from $R_1$ to $R_2$ earth radii. The strength of the sheet is denoted by the field magnitude, $B_{CS}$, produced immediately adjacent to the sheet.

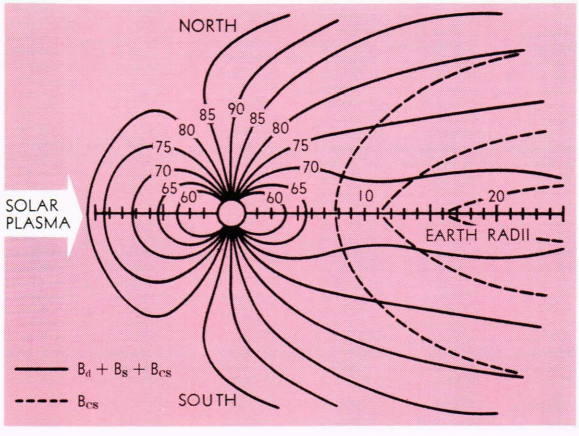


**Fig. 6—Solid lines show resultant field configuration in the noon-midnight meridian which best fits the experimental observations. Dashed lines show field lines due to the current sheet. The current sheet shown here commences at 10 earth radii, extends to 40 earth radii and has a strength of 40 γ adjacent to the sheet. Current flow is out of the paper. Other current sheet parameters are discussed in the text.**

We show in Fig. 5 the comparison of the experimental and theoretical values of the latitude shift, using the magnetic field models described above. The curve denoted $B_d + B_S$ is the original field of Mead[8] and is seen to remain well below the experimental values at all latitudes. The addition of a tail field as strong as 60γ ($1\gamma = 10^{-5}$ gauss) is not sufficient to explain the experimental observations. This value of $B_T$ is already far larger than observations.[10]

We do see, however, that the addition of a current sheet extending from 10 to 40 earth radii and producing a 40-γ field adjacent to the sheet does fit the data. This field configuration is shown in Fig. 6. We see that it is an "open" configuration in the sense that high-latitude field lines do not connect at the equator, i.e. they are pulled out a considerable distance into the tail.

The radial extent of 10 to 40 earth radii and the strength of 40γ adjacent to the sheet are somewhat arbitrary. Table II lists other combinations

TABLE II
CURRENT SHEET PARAMETERS YIELDING FITS TO THE EXPERIMENTAL OBSERVATIONS

| *Front Edge of Current Sheet, $R_1$ (earth radii)* | *Rear Edge of Current Sheet, $R_2$ (earth radii)* | *Field Strength Adjacent to Sheet (γ)* |
|---|---|---|
| 10 | 40 | 40 |
| 8 | 40 | 33 |
| 8 | 100 | 23 |

of these parameters that will also fit the data of Fig. 3. Eventually a more appropriate current distribution possessing the radial dependence implied by the observations of IMP 1,[10] should be used. Nonetheless, this analysis indicates that the nightside geomagnetic field is an open configuration (in the sense described above) and that the current sheet parameters required to fit the trapped electron data are in quite good agreement with the direct observations available in the nightside magnetic field. While the field directions depicted in Fig. 6 are in good agreement with the observations, the field magnitudes listed in Table II are, in general, somewhat larger than the reported measurements.[10] This may be owing to the crudeness of the current sheet and/or neglect of the effects of a ring current.

The existence of a current sheet in the magnetospheric tail, as shown in Fig. 6, leads to a region of zero magnetic field intensity (a neutral surface) separating the anti-solar-directed fields in the southern hemisphere from the solar-directed fields of the northern hemisphere. Such a neutral surface, along with the solar- and anti-solar-directed fields, has been observed by instruments aboard the IMP 1 satellite.[10] The field configuration of Fig. 6, as determined by trapped-electron behavior at 1100 km, is also very similar to recent field models proposed on theoretical grounds.[11,12]

As the data from *1963 38C* were obtained within 8° of the noon-midnight meridian, the truncated semi-infinite current sheet shown in Fig. 6 does yield valid comparisons with the experimental observations. However, for a more realistic three-dimensional view of the plasma currents in the magnetospheric tail, we reproduce the results of Axford *et al.*[12] in Fig. 7. Here the current flow in the tail is visualized by taking a cross section through the tail as seen from the earth. The current sheet used in Fig. 6 is seen in the center of Fig. 7, along with the flow required by the observed magnetic field topology.

The nightside trapping boundary, as defined by field-line closure, occurs at 1100 km at a latitude of 67° in the model of Fig. 6. This is in good agreement with the observed nightside trapping boundary of ≈ 67° for both 40-kev and 280-kev electrons.

Furthermore, recent results[13] indicate that the magnitude of the tail field near the current sheet, $B_{CS}$, increases during the development of the main phase of magnetic storm. Such an increase in $B_{CS}$ will increase the distortions, as shown in Fig. 6, and will result in a southward movement of the nightside trapping boundary because of formerly closed lines being extended into the tail region. Observations of 280-kev electrons from satellite *1963 38C*[6] show that during periods of intense magnetic activity the nightside trapping boundary does indeed move southward approximately 2 to 3° and results in a doubling of the quiet-time latitude shifts.

These results indicate that during periods of magnetic quiet, energetic electrons in the outer zone drift in a distorted magnetic field under the conservation of the adiabatic invariants. This presents a physically pleasing concept of the outer radiation zone and does not require the introduction of acceleration and/or injection mechanisms to explain the quiet-time behavior.

With this understanding of the quiet-time properties of the outer radiation zone, one has hopes of beginning to understand some of the storm-time behavior. Such studies are in progress.

Unfortunately space does not permit listing all those who participated in the project that resulted in the launch of satellite *1963 38C*. However, we are glad to have this opportunity of expressing to all our appreciation for a job well done. Special acknowledgment and appreciation are due Drs. C. O. Bostrom and A. M. Smith of APL, and Mr. H. P. Lie, formerly of APL and now of Bell Telephone Laboratories, for their invaluable assistance.

[11] A. J. Dessler and R. D. Juday, "Configuration of Auroral Radiation in Space," *Planetary Space Science*, **13**, 1965, 63–72.

[12] W. I. Axford, H. E. Petschek and G. L. Siscoe, "Tail of the Magnetosphere," *J. Geophys. Res.*, **70**, 1965, 1231–1236.

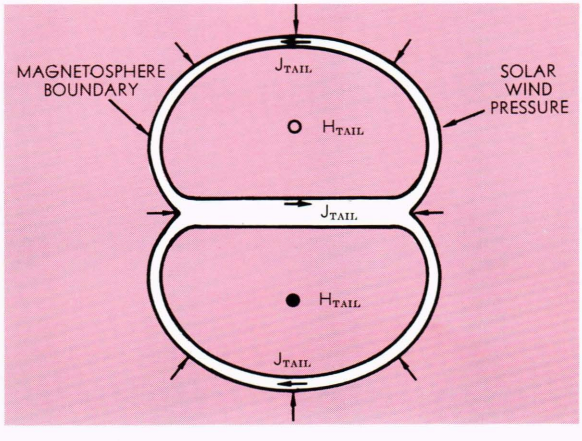


**Fig. 7—A cross section through the magnetosphere tail is seen from the earth, showing the topology of the tail current system. (From Ref. 12, courtesy, *Journal of Geophysical Research*.)**

[13] K. W. Behannon, N. F. Ness, C. S. Scearce, J. B. Seek, and J. M. Wilcox, "Summary of Results from the IMP Magnetic Field Experiment," *Trans. Am. Geophys. Union*, **46**, Mar. 1965, Paper No. 36.